

# UC Riverside

## UC Riverside Previously Published Works

### Title

Targeted Proteomic Approaches for Proteome-Wide Characterizations of the AMP-Binding Capacities of Kinases.

### Permalink

<https://escholarship.org/uc/item/5z66013j>

### Journal

Journal of Proteome Research, 21(8)

### Authors

Miao, Weili  
Yin, Jiekai  
Porter, Douglas  
et al.

### Publication Date

2022-08-05

### DOI

10.1021/acs.jproteome.2c00225

Peer reviewed



# HHS Public Access

Author manuscript

*J Proteome Res.* Author manuscript; available in PMC 2023 August 05.

Published in final edited form as:

*J Proteome Res.* 2022 August 05; 21(8): 2063–2070. doi:10.1021/acs.jproteome.2c00225.

## Targeted Proteomic Approaches for Proteome-Wide Characterizations of the AMP-Binding Capacities of Kinases

**Weili Miao,**

Department of Chemistry, University of California, Riverside, California 92521, United States;  
Program in Epithelial Biology, Stanford University School of Medicine, Stanford, California 94305,  
United States

**Jiekai Yin,**

Environmental Toxicology Graduate Program, University of California, Riverside, California 92521,  
United States

**Douglas F. Porter,**

Program in Epithelial Biology, Stanford University School of Medicine, Stanford, California 94305,  
United States

**Xiaogang Jiang,**

Department of Chemistry, University of California, Riverside, California 92521, United States

**Paul A. Khavari,**

Program in Epithelial Biology, Stanford University School of Medicine, Stanford, California 94305,  
United States

**Yinsheng Wang**

Department of Chemistry and Environmental Toxicology Graduate Program, University of  
California, Riverside, California 92521, United States

### Abstract

Kinases play important roles in cell signaling, and adenosine monophosphate (AMP) is known to modulate cellular energy homeostasis through AMP-activated protein kinase (AMPK). Here, we explored novel AMP-binding kinases by employing a desthiobiotin-conjugated AMP acyl-

---

**Corresponding Author: Yinsheng Wang** – Department of Chemistry and Environmental Toxicology Graduate Program, University of California, Riverside, California 92521, United States; Yinsheng.Wang@ucr.edu.

Author Contributions

W.M. and J.Y. contributed equally.

Supporting Information

The Supporting Information is available free of charge at <https://pubs.acs.org/doi/10.1021/acs.jproteome.2c00225>.

Supplementary Materials and Methods; Figure S1, ESI-MS of desthiobiotin-AMP probe; and Figure S2, AMP binds to MEK2 competitively with ATP (PDF)

Table S1, desthiobiotin sites identified by AMP- and ATP-affinity pull-down (XLSX)

Table S2, AMP/ATP ratios of ATP/AMP probe-enriched kinases from protein pull-down and LC-PRM analysis (XLSX)

Table S3, AMP/ATP ratios of ATP/AMP probe-enriched kinases from peptide pull-down and LC-MRM analysis (XLSX)

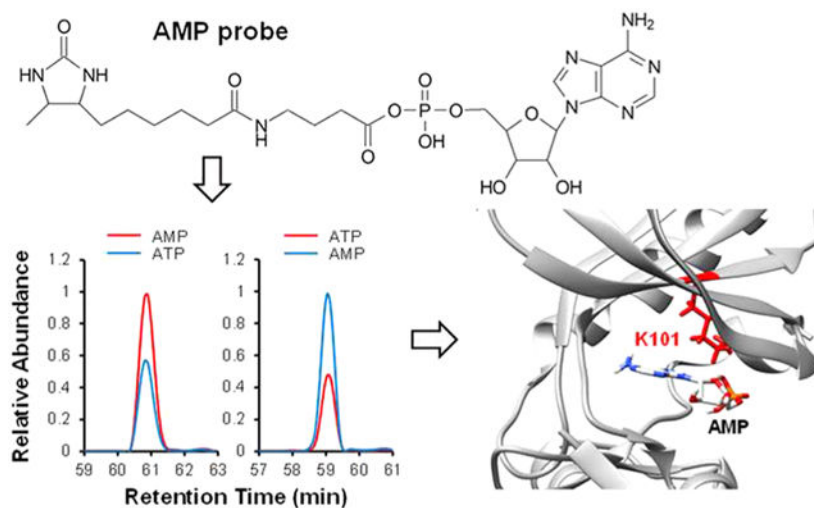
All the raw LC-MS/MS files were deposited into PeptideAtlas with the identifier number of PASS01735 (<http://www.peptideatlas.org/PASS/PASS01735>).

The authors declare no competing financial interest.

Complete contact information is available at: <https://pubs.acs.org/10.1021/acs.jproteome.2c00225>

phosphate probe to enrich efficiently AMP-binding proteins. Together with a parallel-reaction monitoring-based targeted proteomic approach, we uncovered 195 candidate AMP-binding kinases. We also enriched desthiobiotin-labeled peptides from adenine nucleotide-binding sites of kinases and analyzed them using LC-MS/MS in the multiple-reaction monitoring mode, which resulted in the identification of 44 peptides derived from 43 kinases displaying comparable or better binding affinities toward AMP relative to adenosine triphosphate (ATP). Moreover, our proteomic data revealed a potential involvement of AMP in the MAPK pathway through binding directly to the relevant kinases, especially MEK2 and MEK3. Together, we revealed the AMP-binding capacities of a large number of kinases, and our work built a strong foundation for understanding how AMP functions as a second messenger to modulate cell signaling.

## Graphical Abstract



Adenosine monophosphate (AMP) is produced from the hydrolysis of adenosine diphosphate (ADP) or adenosine triphosphate (ATP) and consumed by its conversion to ADP by adenylate kinase (AK).<sup>1</sup> AMP is present in cells in all domains of life and plays important roles in numerous cellular metabolic processes.<sup>2</sup> The cellular ATP/AMP ratio is generally maintained at approximately 100/1, and its perturbation is a rheostat of cellular energy status.<sup>3</sup> An elevated concentration of AMP activates AMP-activated protein kinase (AMPK) to maintain energy homeostasis in cells.<sup>4</sup>

So far only two groups of kinases are known to be activated by AMP, namely, AMPK and 6-phosphofructokinase (PFK), where AMPK is the best-known AMP-binding protein. AMPK is switched on by increases in cellular AMP concentration through three mechanisms, all of which are antagonized by ATP: (a) promotion of phosphorylation of Thr172 by upstream activating kinases; (b) inhibition of Thr172 dephosphorylation by phosphatases; and (c) allosteric activation of the phosphorylated kinase.<sup>5</sup> Given the crucial roles of kinases in modulating cell signaling, proliferation, and metabolism,<sup>6</sup> it is important to examine whether there are other kinases that can bind to AMP and respond to cellular AMP/ATP ratio.

In the present study, we synthesized a desthiobiotin-tagged AMP acyl-phosphate probe and employed this probe (Figures 1a and S1), together with a previously reported desthiobiotin-conjugated ATP probe, which exhibits high specificity in reacting with lysine residues at the ATP-binding pockets of proteins,<sup>7,8</sup> to assess the AMP-binding capacities of kinases at the whole proteome scale. We first examined the relative efficiencies of these two probes in labeling proteins in the lysate of HEK293T cells (Figure 1b). After the labeling reactions, the protein mixtures were reduced, alkylated, and digested with trypsin. The biotinylated peptides in the mixture were enriched with avidin agarose and subjected to LC-MS/MS analyses in the data-dependent acquisition (DDA) mode. Consistent with the fact that there are numerous ATP-binding proteins in cells, our results showed that the ATP-affinity probe led to the identification of many more desthiobiotin-labeled peptides and proteins than the AMP-affinity probe (Figure 1c, Table S1). Furthermore, labeling with the ATP probe conferred much better enrichment of ATP-binding proteins and ATPases than the AMP probe (Figure 1d). Nevertheless, the AMP probe still facilitated the identification of appreciable numbers of ATP-binding proteins and ATPases (Figure 1d).

We next employed the aforementioned desthiobiotin-conjugated ATP and AMP probes, together with stable isotope-labeling by amino acids in cell culture (SILAC),<sup>9</sup> To examine the relative efficiencies of these two probes in labeling kinase proteins in the lysate of HEK293T cells (Figure 1e). After labeling, the desthiobiotin-conjugated proteins were enriched using avidin agarose and digested with trypsin, and the ensuing peptides were subjected to LC-MS/MS analysis in the parallel-reaction monitoring (PRM) mode. In this regard, we used a previously developed PRM kinome library, which contains 1050 unique tryptic peptides derived from 478 non-redundant human kinases, including 395 protein kinases, 21 lipid kinases, and 62 other kinases, and covers approximately 80% of the human protein kinome.<sup>10–17</sup>

Our scheduled LC-PRM analysis with forward and reverse SILAC-labeling led to the quantification of 295 kinases (Figure 2, Table S2). The quantification results showed that the AMP probe was not as effective as the ATP probe in enriching most kinases (Figure 2, Table S2), which is not surprising viewing that most kinases employ ATP as the phosphate group donor for substrate phosphorylation. Interestingly, the two groups of known AMP-activated kinases, AMPK and PFK, display similar enrichments with the use of desthiobiotin-conjugated AMP and ATP probes (Figure 3a). Since AMP/ATP probe-labeling ratios ranged from 0.83 to 1.37 for AMPK and PFK, we employed a cutoff ratio of 0.83 for considering a kinase to have AMP-binding capacity. With this criterion, 195 kinases exhibit AMP-binding capacity. The Kyoto Encyclopedia of Genes and Genomes (KEGG) pathway analysis<sup>18</sup> suggested a high enrichment of the insulin and MAPK signaling pathways for these candidate AMP-binding kinases (Figure 3b).

MAP2K2, a.k.a. MEK2, is an important kinase involved in insulin signaling and MAPK pathways.<sup>19</sup> MEK2 was identified as an AMP-binding protein in our data set with similar binding capacities toward AMP and ATP (Figures 3c and S2a). Autodocking with UCSF Chimera<sup>20</sup> predicted AMP binding to the ATP-binding pocket of MEK2, with the best predicted binding free energy being  $-7.3$  kcal/mol (Figures 3 and S2b), which is indicative of a “valid” binding event.<sup>21</sup> We also employed microscale thermophoresis (MST) to

quantify the binding affinity of MEK2 toward AMP. The result showed a strong interaction between recombinant MEK2 protein and AMP (Figures 3e and S2c,  $K_d = 0.56 \mu\text{M}$ ), which is approximately 2-fold stronger than the corresponding interaction with ATP (Figure 3e,  $K_d = 1.33 \mu\text{M}$ ). In addition, the binding of ATP to MEK2 was decreased by more than 10-fold in the presence of a cellular concentration of AMP ( $10 \mu\text{M}$ , Figure 3f),<sup>3</sup> suggesting the competitive binding of ATP and AMP with MEK2. This finding of MEK2's competitive binding to AMP and ATP is reminiscent of previous observations made for AMPK and PFK.<sup>5,22</sup>

To further explore the competitive binding of kinases toward AMP and ATP, we applied our recently developed kinome MRM library, which includes 818 unique peptides representing 474 distinct human kinases,<sup>7</sup> together with AMP/ATP acylphosphate probes and LC-MRM analysis, to assess quantitatively the AMP-binding capacities of the ATP-binding pockets of kinases (Figure 4a). In this vein, our initial MRM kinome library incorporated isotope-coded ATP-affinity probes for peptide quantification.<sup>8,23</sup> To obviate the need of synthesizing the stable isotope-labeled desthiobiotin-AMP probe, we adapted the MRM kinome library by incorporating SILAC-based quantification, which involved the conversion of MRM transitions of heavy isotope-labeled linker-containing, desthiobiotin-modified peptides to those of the corresponding peptides with heavy isotope-labeled amino acids, i.e., [<sup>13</sup>C<sub>6</sub>, <sup>15</sup>N<sub>2</sub>]-lysine and [<sup>13</sup>C<sub>6</sub>]-arginine. By using the revised version of the MRM kinome library and SILAC, we were able to quantify 406 desthiobiotin-labeled tryptic peptides derived from 279 kinases (Table S3). Among them, 44 desthiobiotin-labeled peptides from 43 kinases exhibited AMP/ATP ratios of over 0.67 (Table 1), indicating comparable or stronger binding affinities of these kinases toward AMP vs ATP. The KEGG pathway analysis of the 43 candidate AMP-binding kinases reveals the MAPK pathway as the most enriched pathway, which are accompanied by pathways known to be regulated by AMP, i.e., the FoxO, Rap1, and AMPK pathways (Figure 4b),<sup>24–26</sup> suggesting that AMP might bind to and regulate kinases in the MAPK pathway. Among these 43 proteins, three are known AMP-binding proteins, i.e., PRKAG1 (a.k.a. AMPK  $\gamma$ 1), PRKAG2 (a.k.a. AMPK  $\gamma$ 2), and PFKP (Table 1). In this vein, Lys161 in AMPK  $\gamma$ 1 was labeled with desthiobiotin, which is consistent with a previous X-ray crystal structure study showing that the corresponding lysine, i.e., Lys169, in rat AMPK  $\gamma$ 1 is involved in binding with the phosphate group in AMP.<sup>27</sup> This result indicates the effectiveness of our approach in revealing the AMP-binding sites of kinases. Next, we investigated the 44 AMP-binding sites for motif enrichment by Multiple Em for Motif Elicitation (MEME). MEME identified a highly specific AMP-binding motif of VAxK (Figure 4c), which is present in more than 50% of the enriched peptides (Figure S2d). There are three known ATP-binding motifs, VAxK, HRDxK, and GxxxxGK ('x' represents any of the 20 natural amino acids),<sup>28</sup> among which the VAxK motif interacts with the  $\alpha$  and  $\beta$  phosphates of ATP to anchor and orient ATP.<sup>29</sup> Thus, the enrichment of the VAxK-motif is in keeping with the fact that AMP only carries an  $\alpha$  phosphate.

As mentioned above, we were able to enrich peptides from the AMP-binding sites of AMPK  $\gamma$ 1 and AMPK  $\gamma$ 2 with similar binding affinities toward ATP and AMP (Figure 4d, Table 1), validating the ability of our approach in uncovering novel AMP-binding kinases together with their binding sites. For the above-mentioned MAPK pathway, we identified

not only MEK2 but also other kinase proteins in the MAPK pathway, e.g., MEK3 (a.k.a. MAP2K3), RPS6KA4, MAP3K2, MAP4K2, MAP3K3, INSR, AKT3, IRAK4, EGFR, MAP3K11, and STK3, as candidate AMP-binding kinases. Among these kinases, MEK3 exhibits an ~2-fold stronger binding to AMP than ATP (Figure 4e). Similar to MEK2, AMP binds to the ATP-binding site of MEK3 (Uniprot), where the desthiobiotin-labeled K93 is located in the ATP-binding pocket. Importantly, K93 in MEK3 is the homologous lysine to K101 in MEK2, further indicating that AMP binds to the ATP-binding domain of both MEK2 and MEK3.

The PRM and MRM targeted proteomic methods provide the quantitative information for 295 and 278 kinases, respectively, with 156 kinases being commonly quantified with both approaches (Figure 4f). By comparing the kinases with AMP-binding capacities obtained from PRM analysis and kinases with AMP-binding capacities in the ATP-binding domains from MRM analysis, we found an overlap of 16 kinases (Figure 4f), including the known AMP-activated kinases (i.e., PRKAG1, PRKAG2 and PFKP, Figure 4g). In addition, kinases such as INSR, CDK2, SYK, SMG1, NEK7, CSK, TNIK, IRAK4, CDK7, BCR, LATS1, MAP4K5, and AKT3 performed similarly as the three known AMP-activated kinases (Figure 4g), suggesting that they are potential AMP-activated kinases.

It is worth discussing the moderate overlap between the data acquired from pull-down at the protein (for PRM analysis) and peptide (for MRM analysis) levels. In this vein, some kinase proteins (e.g., MEK2) are in the PRM library but not the MRM library, and vice versa is also true. In particular, our PRM and MRM libraries encompass 478 and 474 kinase proteins, respectively, and 350 kinase proteins are commonly present in the two libraries.<sup>10,30</sup> In addition, the MRM library was established based on affinity pull-down using the ATP acyl-phosphate probe, and some AMP-binding proteins may not bind strongly to ATP and hence are not included in the MRM library. On the other hand, the majority of shotgun proteomic data used for constructing the PRM library were acquired from the analyses of tryptic digestion mixtures of whole-cell protein lysates without enrichment; hence, low-abundance kinases may escape the detection and are not included in the PRM library.

In summary, we synthesized a desthiobiotin-AMP acyl-phosphate probe. By employing this probe and a previously synthesized desthiobiotin-ATP probe, together with a PRM-based targeted proteomics approach, we uncovered 195 kinases with potential AMP-binding capacity. Additionally, our analysis of the desthiobiotin-labeled peptides from ATP-binding sites of kinases led to the discovery of 44 peptides from 43 kinases manifesting comparable or stronger binding toward AMP relative to ATP. We also uncovered VAXK as the AMP-binding motif for kinases. Additionally, our work suggests the potential involvement of AMP in the MAPK pathway by binding directly to the relevant kinases, especially MEK2 and MEK3. Together, our chemoproteomic approaches revealed AMP-binding capacities for a large number of kinases, and our work built a strong foundation for understanding how AMP functions as a second messenger and a regulator of cell signaling.

## Supplementary Material

Refer to Web version on PubMed Central for supplementary material.

## ACKNOWLEDGMENTS

This work was supported by the National Institutes of Health (R01 CA210072).

## REFERENCES

- (1). Amiri M; Conserva F; Panayiotou C; Karlsson A; Solaroli N The human adenylate kinase 9 is a nucleoside mono- and diphosphate kinase. *Int. J. Biochem* 2013, 45, 925–931.
- (2). Jauker M; Griesser H; Richert C Spontaneous Formation of RNA Strands, Peptidyl RNA, and Cofactors. *Angew. Chem., Int. Ed. Engl* 2015, 54, 14564–14569. [PubMed: 26435376]
- (3). Hardie DG Keeping the home fires burning†: AMP-activated protein kinase. *J. R. Soc. Interface* 2018, 15, 20170774. [PubMed: 29343628]
- (4). Kim J; Yang G; Kim Y; Kim J; Ha J AMPK activators: mechanisms of action and physiological activities. *Exp. Mol. Med* 2016, 48, No. e224. [PubMed: 27034026]
- (5). Gowans GJ; Hardie DG AMPK: a cellular energy sensor primarily regulated by AMP. *Biochem. Soc. Trans* 2014, 42, 71–75. [PubMed: 24450630]
- (6). Lemmon MA; Schlessinger J Cell signaling by receptor tyrosine kinases. *Cell* 2010, 141, 1117–1134. [PubMed: 20602996]
- (7). Miao W; Xiao Y; Guo L; Jiang X; Huang M; Wang Y A high-throughput targeted proteomic approach for comprehensive profiling of methylglyoxal-induced perturbations of the human kinome. *Anal. Chem* 2016, 88, 9773–9779. [PubMed: 27626823]
- (8). Xiao Y; Guo L; Wang Y A targeted quantitative proteomics strategy for global kinome profiling of cancer cells and tissues. *Mol. Cell. Proteomics* 2014, 13, 1065–1075. [PubMed: 24520089]
- (9). Ong SE; Blagoev B; Kratchmarova I; Kristensen DB; Steen H; Pandey A; Mann M Stable isotope labeling by amino acids in cell culture, SILAC, as a simple and accurate approach to expression proteomics. *Mol. Cell. Proteomics* 2002, 1 (5), 376–86. [PubMed: 12118079]
- (10). Miao W; Guo L; Wang Y Imatinib-induced changes in protein expression and ATP-binding affinities of kinases in chronic myelocytic leukemia cells. *Anal. Chem* 2019, 91, 3209–3214. [PubMed: 30773012]
- (11). Miao W; Li L; Liu X; Qi TF; Guo L; Huang M; Wang Y A targeted quantitative proteomic method revealed a substantial reprogramming of kinome during melanoma metastasis. *Sci. Rep* 2020, 10, 2485. [PubMed: 32051510]
- (12). Miao W; Li L; Wang Y High-throughput targeted quantitative analysis of the interaction between HSP90 and kinases. *Anal. Chem* 2019, 91, 11507–11509. [PubMed: 31476117]
- (13). Miao W; Wang Y Targeted quantitative kinome analysis identifies PRPS2 as a promoter for colorectal cancer metastasis. *J. Proteome Res* 2019, 18, 2279–2286. [PubMed: 30908912]
- (14). Miao W; Wang Y Quantitative interrogation of the human kinome perturbed by two BRAF inhibitors. *J. Proteome Res* 2019, 18, 2624–2631. [PubMed: 30994353]
- (15). Miao W; Yuan J; Li L; Wang Y Parallel-reaction monitoring-based proteome-wide profiling of differential kinase protein expression during prostate cancer metastasis in vitro. *Anal. Chem* 2019, 91, 9893–9900. [PubMed: 31241916]
- (16). Miao W; Yang Y-Y; Wang Y Quantitative Proteomic Analysis Revealed Broad Roles of N6-Methyladenosine in Heat Shock Response. *J. Proteome Res* 2021, 20, 3611–3620. [PubMed: 34043365]
- (17). Miao W; Bade D; Wang Y Targeted Proteomic Analysis Revealed Kinome Reprogramming during Acquisition of Radio-resistance in Breast Cancer Cells. *J. Proteome Res* 2021, 20, 2830–2838. [PubMed: 33739118]

- (18). Kanehisa M; Furumichi M; Tanabe M; Sato Y; Morishima K KEGG: new perspectives on genomes, pathways, diseases and drugs. *Nucleic Acids Res.* 2017, 45 (D1), D353–D361. [PubMed: 27899662]
- (19). Carel K; Kummer JL; Schubert C; Leitner W; Heidenreich KA; Draznin B Insulin Stimulates Mitogen-activated Protein Kinase by a Ras-independent Pathway in 3T3-L1 Adipocytes \*. *J. Biol. Chem* 1996, 271, 30625–30630. [PubMed: 8940037]
- (20). Pettersen EF; Goddard TD; Huang CC; Couch GS; Greenblatt DM; Meng EC; Ferrin TE UCSF Chimera—A visualization system for exploratory research and analysis. *J. Comput. Chem* 2004, 25 (13), 1605–1612. [PubMed: 15264254]
- (21). Lee HS; Jo S; Lim H-S; Im W Application of binding free energy calculations to prediction of binding modes and affinities of MDM2 and MDMX inhibitors. *J. Chem. Inf. Model* 2012, 52, 1821–1832. [PubMed: 22731511]
- (22). Kamp G; Schmidt H; Stypa H; Feiden S; Mahling C; Wegener G Regulatory properties of 6-phosphofructokinase and control of glycolysis in boar spermatozoa. *Reprod* 2007, 133, 29–40.
- (23). Xiao Y; Guo L; Wang Y Isotope-coded ATP probe for quantitative affinity profiling of ATP-binding proteins. *Anal. Chem* 2013, 85 (15), 7478–86. [PubMed: 23841533]
- (24). Bryn T; Mahic M; Enserink JM; Schwede F; Aandahl EM; Taskén K The Cyclic AMP-Epac1-Rap1 Pathway Is Dissociated from Regulation of Effector Functions in Monocytes but Acquires Immunoregulatory Function in Mature Macrophages. *J. Immunol* 2006, 176, 7361. [PubMed: 16751380]
- (25). Greer EL; Banko MR; Brunet A AMP-activated protein kinase and FoxO transcription factors in dietary restriction-induced longevity. *Ann. N.Y. Acad. Sci* 2009, 1170, 688–692. [PubMed: 19686213]
- (26). Mihaylova MM; Shaw RJ The AMPK signalling pathway coordinates cell growth, autophagy and metabolism. *Nat. Cell Biol* 2011, 13, 1016–1023. [PubMed: 21892142]
- (27). Xiao B; Heath R; Saiu P; Leiper FC; Leone P; Jing C; Walker PA; Haire L; Eccleston JF; Davis CT; Martin SR; Carling D; Gamblin SJ Structural basis for AMP binding to mammalian AMP-activated protein kinase. *Nature* 2007, 449 (7161), 496–500. [PubMed: 17851531]
- (28). Xiao Y; Guo L; Jiang X; Wang Y Proteome-Wide Discovery and Characterizations of Nucleotide-Binding Proteins with Affinity-Labeled Chemical Probes. *Anal. Chem* 2013, 85, 3198–3206. [PubMed: 23413923]
- (29). Fabbro D; Cowan-Jacob SW; Moebitz H Ten things you should know about protein kinases: IUPHAR Review 14. *Br. J. Pharmacol* 2015, 172, 2675–2700. [PubMed: 25630872]
- (30). Miao W; Wang Y Chapter 7 - Mass spectrometry for human kinome analysis. In *Advances in Chemical Proteomics*; Yao X, Ed.; Elsevier: 2022; pp 191–216, DOI: 10.1016/B978-0-12-821433-6.00001-5.



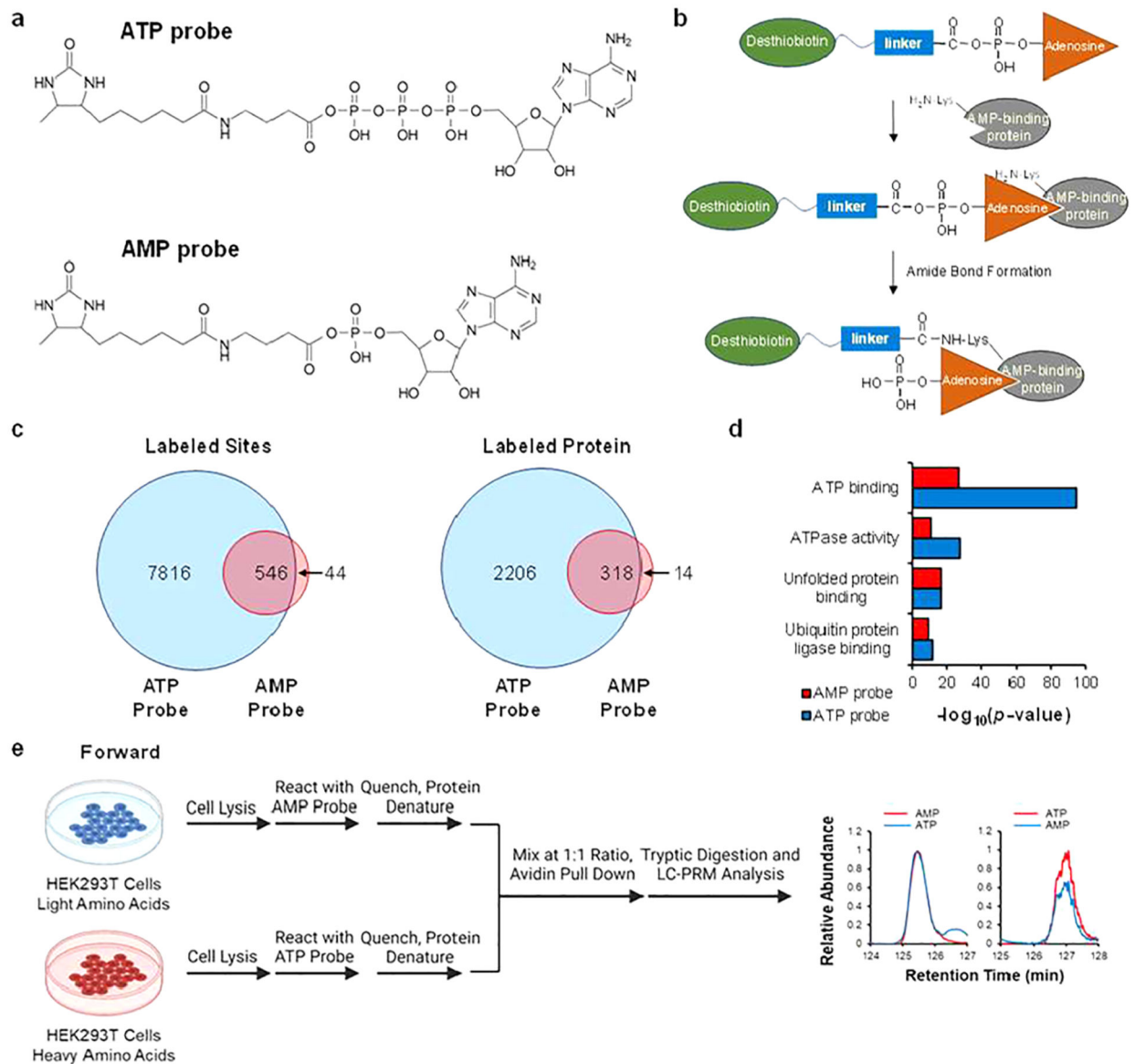


**Figure 1.**

An AMP acyl-phosphate probe-based chemoproteomic method for interrogating the AMP-binding capacities of kinases. (a) The chemical structures of the ATP- (top) and AMP- (bottom) affinity probes. (b) The working principle of the AMP-affinity probe. (c) Venn diagrams illustrating the comparisons of the numbers of desthiobiotin-labeled sites (left) and desthiobiotin-labeled proteins (right) obtained from ATP- and AMP-affinity probe pull-down followed by desthiobiotinylated peptide enrichment and shotgun proteomic analysis. (d) Gene ontology analysis of the desthiobiotin-labeled proteins identified from ATP- and AMP-affinity probe pull-downs, where the  $p$ -values were exported from DAVID functional annotation. (e) A SILAC and PRM-based targeted proteomic approach for proteome-wide identification of AMP-binding kinases. Displayed here is the forward SILAC-labeling experiment. In the reverse SILAC-labeling experiment, the light- and heavy-labeled lysates are incubated with the ATP and AMP probes, respectively.

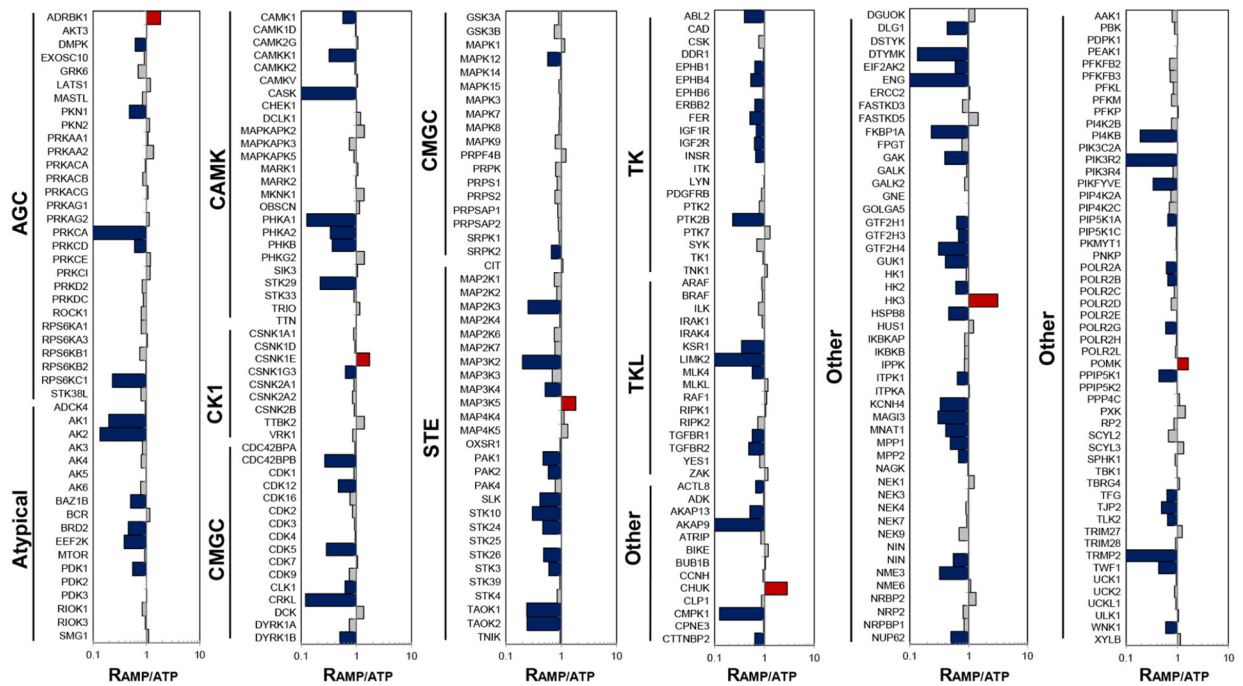


**Figure 2.**

Differential AMP- and ATP-binding capabilities of kinases. The ratios represent the proteins enriched by the AMP- vs ATP-affinity probe from the lysate of HEK293T cells. Plotted are the quantification results from the means of two biological replicates (one forward and one reverse SILAC labeling experiment, see Table S2 for ratios obtained from individual measurements). Blue, red, and gray bars represent those kinases with ratios (AMP/ATP) being <0.67, >1.5, and between 0.67 and 1.5, respectively.

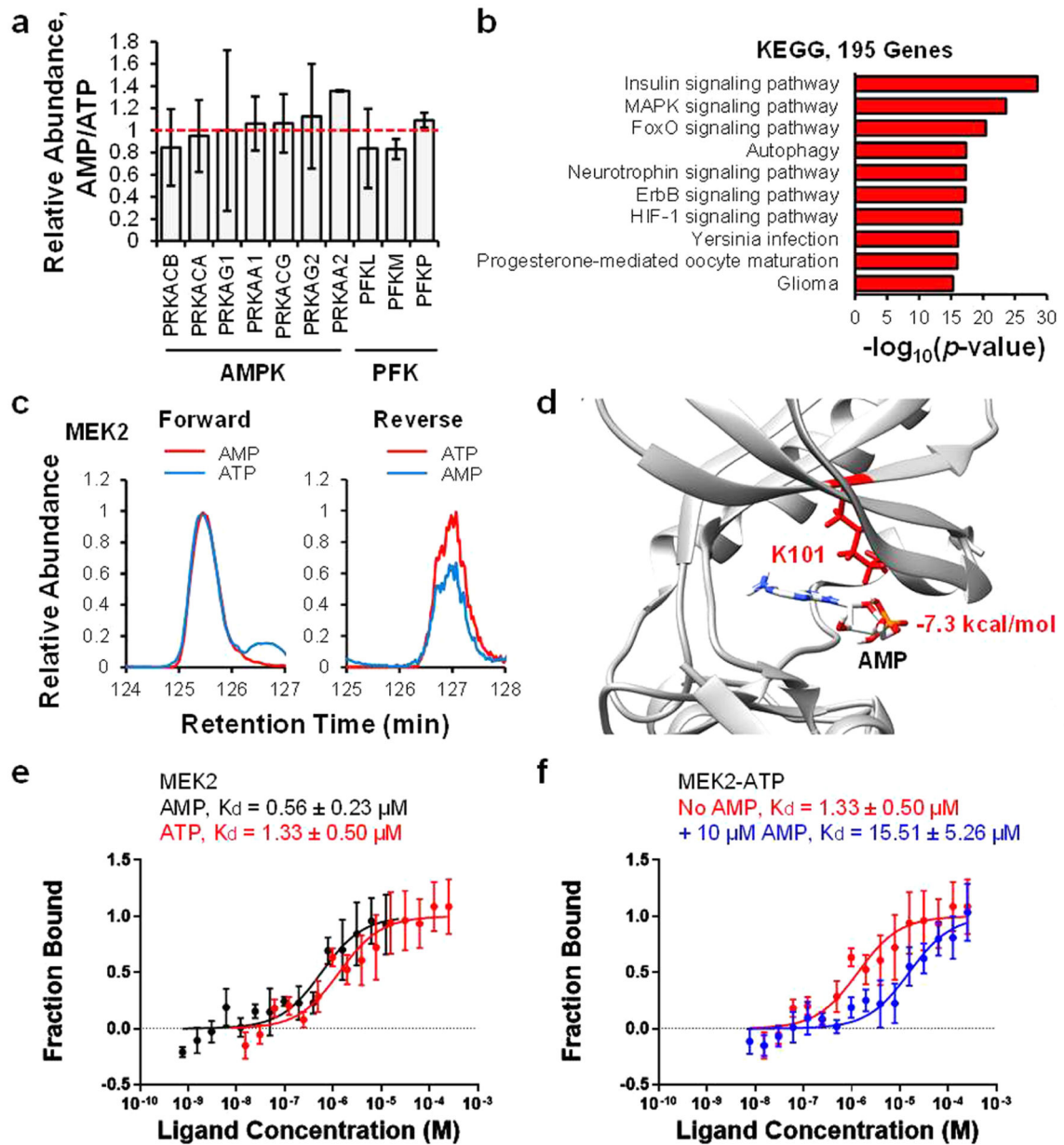


**Figure 3.**

AMP binds to MEK2. (a) The relative ratios of AMPK and PFK proteins enriched from AMP over ATP acyl-phosphate probes and quantified from LC-PRM analyses. (b) KEGG pathway analysis of the kinases with AMP/ATP probe-labeling ratios being  $>0.83$ , where the  $p$ -values were exported from Enrichr. (c) PRM traces for the MEK2 kinase peptide. (d) Molecular docking by UCSF Chimera shows the predicted binding site of AMP to MEK2 (PDB: 1S9I). MST analysis of the binding affinity of MEK2 with ATP or AMP (e) or with ATP in the presence or absence of 10  $\mu\text{M}$  AMP (f).

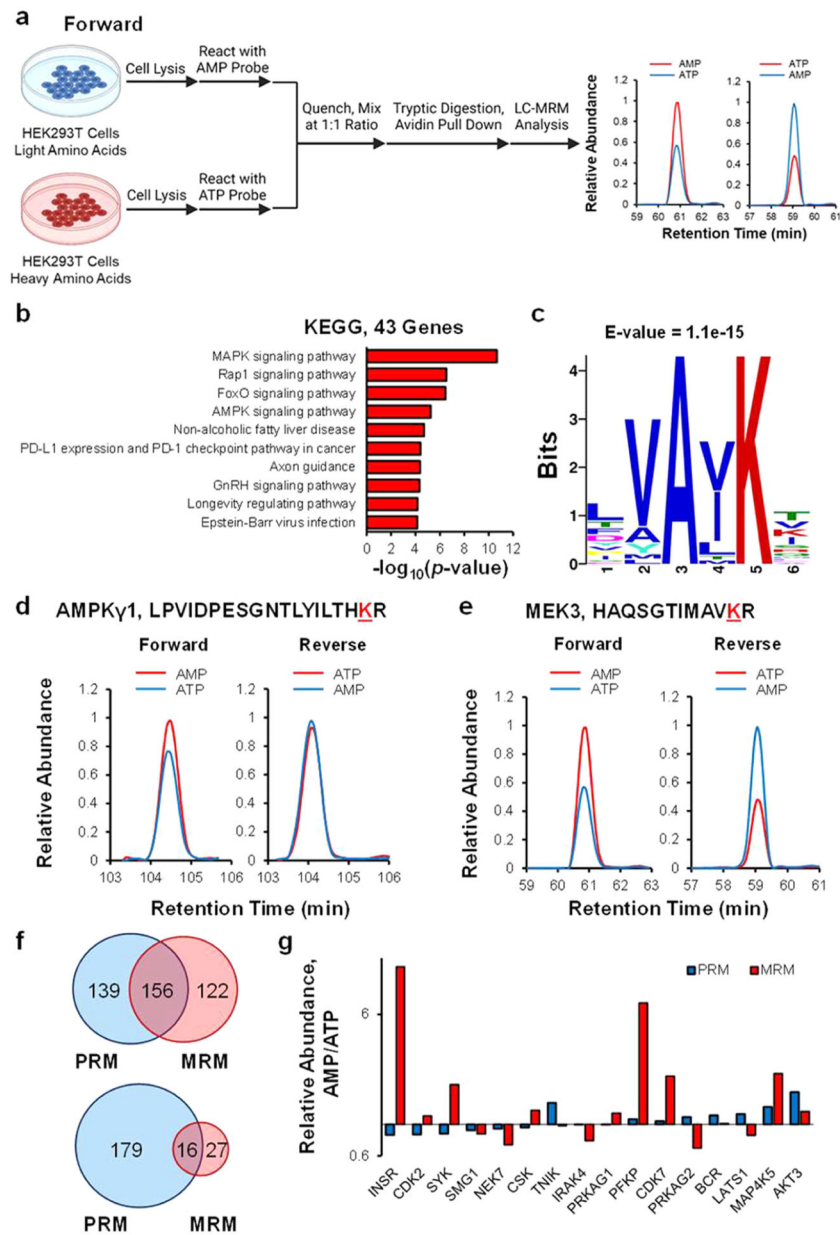


**Figure 4.** Systematic analysis of competitive binding of kinases to AMP and ATP. (a) Experimental strategy for the MRM-based targeted proteomic approach for assessing the competitive binding of kinases toward AMP and ATP, and displayed here is the forward-labeling experiment. (b) KEGG pathway analysis of kinases with AMP/ATP > 0.67, where  $p$ -values were exported from Enrichr. (c) The most enriched motif in desthiobiotin-labeled peptides with AMP/ATP > 0.67. (d) MRM traces of the AMPK  $\gamma$ 1 kinase peptide. (e) MRM traces of the MEK3 kinase peptide. (f) Venn diagrams showing the number of kinases quantified from MRM and PRM experiments (top) and the number of potential AMP-binding kinases

quantified from MRM and PRM (bottom). (g) The enrichment ratios (AMP/ATP-probes) for the 16 candidate AMP-binding kinases commonly quantified from PRM and MRM analyses.

Author Manuscript

Author Manuscript

Author Manuscript

Author Manuscript

Table 1.

A List of Kinases and Their Corresponding Desthiobiotin-Labeled Peptides with AMP/ATP Probe-Labeling Ratios Being  $>0.67^a$

kinases	desthiobiotin-labeled peptides	forward ratio (AMP/ATP)	reverse ratio (AMP/ATP)	av ratio (AMP/ATP)
<b>PRKAG2</b>	LPVIDPISGNALYLTHK#R	0.84	0.52	0.68
NEK7	AACLLDGVVPALK#K	0.76	0.68	0.72
CERT	K#SHFGGPDYEEGPNSLINEEEFFDAVEAALDR	0.65	0.82	0.73
IRAK4	GYVNNTTVAVK#K	0.73	0.81	0.77
EGFR	IPVAIK#ELR		0.79	0.79
LATS1	ALYATK#TLR	0.77	0.91	0.84
MAP4K2	DTVTSELAAVK#IVK	0.88	0.81	0.85
SMG1	SYPYLFK#GLEDLHLDER	0.92	0.79	0.86
RPS6KA4	VLGTGAYGK#VFLVR	0.67	1.05	0.86
DYRK3	QYVALK#MVR		0.87	0.87
PRKD2	DVAVK#VIDK	0.93	0.93	0.93
STK3	ESGQVVAIK#QVPVESDLQEIHK	0.92	0.96	0.94
MAP3K3	ELASK#QVQFDPDSPETSK	1.01	0.90	0.96
TNIK	TGQLAAIK#VMDVVTGDEEBEIKQEINMLK	0.94	1.02	0.98
PKN1	SPLTLEDFK#FLAVLGR	1.12	0.88	1.00
BCR	VAEK#EAVNK	1.07	0.96	1.02
PRKD1	DVAIK#HDK	1.33	0.85	1.09
EPHA1	TVAIK#TLK	1.17	1.03	1.10
CDK2	LTGEVVALK#K	1.08	1.22	1.15
PRKD3	DVAIK#VIDK	1.20	1.12	1.16
FEER	TSVAVK#TCK	1.04	1.33	1.19
<b>PRKAG1</b>	LPVIDPESGNTLYLTHK#R	1.29	1.11	1.20
CSNK1A1L	DIK#PDNFLMGTGR	1.22		1.22
AKT3	TMNDFDYLK#LLGK	1.86	0.61	1.24
CSK	VAVK#CIK	1.20	1.32	1.26
CSNK1G1	NLYTNEYVAIK#LEPIK	2.24	0.67	1.45
MAP3K2	ELAVK#QVQFDPDSPETSK	1.60	1.39	1.49
TSSK2	DLK#CENLLLDK	1.48	1.82	1.65

kinases	desthiobiotin-labeled peptides	forward ratio (AMP/ATP)	reverse ratio (AMP/ATP)	av ratio (AMP/ATP)
MAP3K11	GELVAVK#AAR	1.62	1.72	1.67
RPS6KA4	LYAMK#VLR	1.49	2.00	1.75
MAP2K3	HAQSGTIMAVK#R	1.76	2.04	1.90
SYK	TVAVK#LTK	2.15	1.67	1.91
CDK7	NTNQIVAIK#K	3.05	1.33	2.19
MAP4K5	NVHTGELAAVK#HK	3.03	1.54	2.28
EPHB3	EYFVAIK#TLK	2.80	2.86	2.83
CDC42BPB	NSGTCLFVAVK#R	5.94	3.45	4.69
RIOK1	LNVTDSVINK#VTEK	9.85	1.52	5.68
EPHB2	EIFVAIK#TLK	5.88	5.56	5.72
<b>PKP</b>	NFGTK#ISAR	6.10	8.33	7.22
CSNK1G2	DVK#PENFLVGRPGTK	13.96	3.85	8.90
EPHA7	K#MSSIQTMR	19.01	4.55	11.78
INSR	VAVK#TVNESASLR	9.32	16.67	12.99
FES	ADNTLVAVK#SCR	15.50	12.50	14.00
NUAK2	LVAIK#SIR	11.96	25.00	18.48

<sup>a</sup>Shown are the ratios obtained from two biological replicates (one forward and one reverse). The kinases highlighted in bold are known AMP-binding proteins. "K#" in peptide sequences represents desthiobiotin-labeled lysine.